Advanced Materials Interfaces

ADVANCED MATERIALS INTERFACES Open Access

www.advmatinterfaces.de

RESEARCH ARTICLE OPEN ACCESS

Assessing TiO_2/Chitosan-Based Hydrogels for Water Remediation: Sunlight-Driven Degradation of Antibiotics in Water

Beatrice Cerea[1,2,3] | Giovanni Ribaudo[2,4] | Alessandra Gianoncelli[2,4] | Matteo Ferroni[3,5,6] | Irene Vassalini[1,2,3] | Ivano Alessandri[1,2,3]

[1]Department of Information Engineering (DII), University of Brescia, Brescia, Italy | [2]INSTM, Brescia, Italy | [3]INO-CNR, Brescia, Italy | [4]Department of Molecular and Translational Medicine (DMMT), University of Brescia, Brescia, Italy | [5]Department of Civil, Environmental, Architectural Engineering and Mathematics (DICATAM), University of Brescia, Brescia, Italy | [6]CNR-ISMN Bologna, Bologna, Italy

Correspondence: Ivano Alessandri (ivano.alessandri@unibs.it)

Received: 13 March 2026 | **Revised:** 23 April 2026 | **Accepted:** 10 May 2026

Keywords: chitosan composite hydrogels | emerging organic pollutants | solar photocatalysis | sulfamethoxazole | water treatment

ABSTRACT

The widespread occurrence of pharmaceutical contaminants in aquatic environments requires the development of sustainable and efficient water treatment technologies capable of operating under realistic conditions. In this study, an integrated remediation system based on chitosan hydrogels embedding TiO_2 nanoparticles is investigated, combining pollutant adsorption and photocatalytic degradation within a single, reusable system. The performance of the composite hydrogels was evaluated for the removal of sulfamethoxazole (SMX), selected as a model antibiotic, under simulated and real solar irradiation, using mineral water to reproduce environmentally relevant ionic strength conditions. Structural characterization confirms the effective immobilization of TiO_2 within the hydrogel matrix, ensuring material stability and preventing nanoparticle release into water. The hybrid system exhibits high SMX removal efficiency (>85% for 10^{-5} M SMX solutions) due to the synergistic interplay between adsorption and sunlight-driven photocatalysis, with TiO_2 showing photocatalytic activity under solar irradiation. Moreover, the hydrogels show excellent structural integrity, resistance to microbial colonization and biofouling, and stable performance over multiple adsorption–photocatalysis cycles. These results demonstrate the robustness and practical applicability of TiO_2/chitosan-based hydrogels for solar-driven water remediation and provide a promising platform for the development of advanced multifunctional materials for the treatment of emerging contaminants.

1 | Introduction

The increasing scarcity of clean water, exacerbated by rapid population growth, climate change, and depletion of freshwater resources, has underscored the urgent need for sustainable water purification strategies [1]. Of particular concern are emerging and persistent organic pollutants (EPOPs), such as pharmaceuticals, pesticides, personal care products, dyes, and antibiotics, since they are frequently found in aquatic environments and resist conventional treatment methods. Unfortunately, despite their environmental prevalence, they are still largely unregulated [2, 3]. Several treatment methods have been developed to address the limitations of traditional systems, including advanced oxidation processes (AOPs) [4, 5], membrane-based technologies [6, 7], and composite adsorbents [8–10]. (AOPs) have emerged as particularly promising due to their capacity to degrade a wide range of organic pollutants through the generation of highly reactive species, particularly hydroxyl radicals (•OH) and superoxide

anions (O_2•–), whose formation can be boosted by appropriate catalysts. The use of photocatalysts that can directly operate under solar light and mild conditions is a promising route for making the overall process effective and environmentally sustainable. Titanium dioxide (TiO_2) is widely utilized in photocatalysis for its high oxidative power, photochemical stability, biocompatibility, affordability, and photocatalytic efficiency. However, in the absence of doping or structural defects that can extend the optical absorption in the visible range, TiO_2 has a wide bandgap (3–3.2 eV), which makes it more effective under UV-light irradiation. Moreover, the practical application of TiO_2 in aqueous systems is hindered by challenges related to catalyst recovery, since TiO_2 nanoparticles are difficult to separate from treated water, giving rise to possible secondary contamination and limiting their use on a large scale. To address this drawback, several strategies have been proposed and implemented. For example, our group developed millimetre-sized photocatalytic beads of photocatalytic anatase TiO_2, obtained from alginate through ionotropic gelation, which allowed for a synergistic combination of efficient photocatalysis, recovery, and recyclability [11–13]. Another promising strategy involves the immobilization of TiO_2 within hydrogel matrices [14–16]. This approach not only allows for easier recovery and reuse of the photocatalyst but also enhances the overall treatment efficiency through the simultaneous adsorption and photocatalytic degradation of pollutants, reducing the environmental impact of the remediation method and supporting the development of integrated water purification technologies. More generally, both synthetic and naturally derived hydrogels are garnering ever-increasing attention in water treatment research, because of their cost-effectiveness, recyclability/biodegradability, and versatility. In particular, hydrogels obtained from biomass or bio-waste sources offer unique advantages for the circular economy and sustainability [17–19].

In this context, chitosan-based hydrogels are intensively investigated for capturing/removing a variety of pollutants, ranging from heavy metal ions, polyfluoroalkyl substances (PFAS), and different types of organic dyes and pesticides [18, 19]. Chitosan is a natural biopolymer derived from the deacetylation of chitin, an abundant waste material from the seafood industry, representing a sustainable choice for the development of a hydrogel-based water treatment system [20]. It is biodegradable and biocompatible, with the major benefits of intrinsic antibacterial activity. Furthermore, it permits the incorporation of various functional components into the hydrogel matrix, which enables the design of multifunctional systems with enhanced adsorption and catalytic properties [21].

In this work, we present an integrated system that combines the photocatalytic activity of TiO2 and the adsorption capacity of chitosan hydrogel for the removal of sulfamethoxazole (SMX) from water.

SMX is one of the most utilized sulfonamide-based antibiotics, which are widely used in human and veterinary medicine [22]. SMX is only partially metabolized by living organisms and persists in water systems, contributing to antibiotic resistance by promoting the development of antibiotic-resistant bacteria [23, 24]. This class of contaminants is notably persistent and inadequately removed by standard wastewater treatments, making it a priority target for innovative remediation approaches.

TABLE 1 | Analysis of the mineral water used for the preparation of sulfamethoxazole solutions.

Water temperature at the source	**10.8°C**
pH at the water temperature at the source	7.6
Specific electrical conductivity at 20°C	91 µS/cm
Total dissolved solids (TDS)	60 mg/L
Hardness	5.9
Oxidizability	<0.5 mg/L
Free carbon dioxide at the source	6 mg/L
Contained ions	Concentration (mg/L)
Ca^{2+}	11.2
Mg^{2+}	3.5
Na^{+}	2.0
K^{+}	0.7
H^{+}	50
SO_4^{2-}	5.6
NO_3^{-}	3.8
Cl^{-}	2.0
F^{-}	<0.1
SiO_2	7.1

In this work, we demonstrate that these hybrid composites enable decontamination of mineral water even in the presence of possible ionic interferents under solar light irradiation, operating under mild conditions. Experiments conducted at different SMX concentrations demonstrate that TiO_2 remains active within the hydrogel matrix and under solar irradiation, and the resulting degradation products have been identified and discussed. Furthermore, the recyclability of the hydrogels both as adsorbents and as photocatalysts has been evaluated, together with their performance under real sunlight, showing their potential for practical water treatment applications.

2 | Experimental Section

2.1 | Materials

All reagents were obtained from commercial suppliers and used as received. TiO_2 powder was purchased from Degussa Corporation, chitosan was obtained from Biobasic, sulfamethoxazole, sodium hydroxide (NaOH), acetic Acid (CH_3COOH) were purchased from Sigma–Aldrich. Mineral water, whose chemical analysis is indicated in Table 1, was used for all the experiments.

2.2 | Chitosan-Based Hydrogels Fabrication

A total of 0.9 g of chitosan was dissolved in 30 mL of 5% v/v acetic acid solution under continuous stirring until complete dissolution was achieved. The resulting solution was then poured

into a Petri dish and fully covered with 3 M NaOH to induce physical crosslinking. After 6 h, the hydrogel was thoroughly washed with distilled water until a neutral pH was reached. For the preparation of CH/TiO_2 hydrogels, 0.3 g TiO_2 powder was dispersed in 30 mL of 5% v/v acetic acid to obtain a final concentration of 1% w/v. This loading was selected on the basis of preliminary tests performed using methylene blue as a model pollutant. These experiments showed that a 1% wt TiO_2 loading provided the best overall balance between photocatalytic efficiency, adsorption capability, and the physical characteristics of the hydrogel in terms of handling, structural integrity, and practical usability. To evaluate the potential release of TiO_2 from the CH/TiO_2 hydrogel over time, a hydrogel disk weighing 1.1 ± 0.1 g was immersed in demineralized water, and the solution was subsequently analyzed by a benchtop Total Reflection X-Ray Fluorescence (TXRF) spectrometer (Horizon, G.N.R., Italy). The instrument is equipped with a molybdenum x-ray tube coupled with a W/Si multilayer monochromator to provide a Mo-Kα beam (17.44 keV) for sample excitation. The fluorescence signal generated by the sample was collected by a 40 nm^2 silicon drift detector (KETEK GmbH), featuring a 1 mm graphene window, a collimator, and a polymer film. Measurements were carried out at 40 kV and 15 mA in air using gallium as the internal standard.

2.3 | Raman and FTIR Characterization of the Hydrogels

Raman spectroscopy was performed using a Labram HR-800 μ-spectrometer from Horiba-Jobin Yvon equipped with an optical microscope (BX41; Olympus Optical Co. Ltd.), a 632.8 nm He-Ne laser source, and a CCD detector (Wright Instruments Ltd.). A piece of wet CH and CH/TiO_2 hydrogels was analyzed using a 10× microscope objective with an acquisition time equal to 30 and 120 s. Each measurement has been repeated at least 3 times, on different areas inside the sample.

ATR-FTIR characterization was carried out by acquiring data on powder specimens with a Nicolet Summit Spectrometer (Thermo-Fisher), equipped with the Everest Diamond ATR optics. 64 spectra were acquired for each specimen, with a spectral resolution of 4 cm^{-1}.

2.4 | Adsorption and Photodegradation Tests

The adsorption and photocatalytic efficiency of CH and CH/TiO_2 hydrogels were evaluated by assessing their ability to remove sulfamethoxazole (SMX), considering 10^{-5} and 10^{-3} M solutions in mineral water. In all the experiments, a disk of 1.1 ± 0.1 g of hydrogel was submerged in 5 mL of pollutant solution and kept in the dark overnight without stirring to allow adsorption-desorption equilibrium and to evaluate the adsorption capability of the system. The system was then irradiated with visible light illumination using a solar simulator (Abet Technologies, Sun 2000 Simulator, model: 11 016) equipped with a Xe arc lamp (power: 550 W) illumination intensity of 1 Sun (irradiance: A.M. 1.5 G, spectral match A, working distance: 15 cm, field size: 100 × 100 mm, stability: 1%, uniformity: 1%) or using directly the solar light (*see* data reported in Section S4). The variation of the concentration of SMX over irradiation time was determined by high-performance liquid chromatography analysis (HPLC), using a DionexTM UltiMateTM 3000 Thermo Fisher Scientific S.p.A. (Milan, Italy) instrument equipped with LPG-3400SD quaternary analytical pump, a WPS-3000SL analytical autosampler, a VWD-310 UV–vis detector, and a TCC-3000SD thermostated column compartment. Chromatographic separation was performed using an Agilent Zorbax Eclipse Plus C18 (100 mm × 2.1 mm ID, particle size 1.8 μm); the mobile phase composition was (A) TFA 0,05% and (B) methanol; and the mobile phase flow rate was 0.3 mL/min. The gradient program was as follows: 5% B for 0.5 min., from 5% to 95% B in 10.5 min., 95% B for 1 min., from 95% to 5% B in 1 min. and then 5% B for 2 min. All the analyses were performed at 30°C, and the detection wavelength was set at 230 nm. The calibration curves were built using sulfamethoxazole standard solutions with the following concentrations: 5, 10, 25, 50, 100, 200, 500, and 1000 ng/mL.

All the experiments were performed in triplicate, in order to achieve a significant statistic.

The percentage of adsorbed pollutant was determined using the following equation:

$$\% \text{ adsorbed} = (A_0 - A_t)/A_0 \text{ x } 100 \quad (1)$$

where A_0 is the initial value of absorbance of the analyte, proportional to the initial concentration, and A_t is the value of absorbance measured at time t after leaving the solution in contact with the hydrogel in the dark without stirring.

The degradation efficiency under solar-light illumination was measured every 30 min up to 4 h, and the calculation was made using the following formula:

$$\% \text{ degradation} = (C_0 - C_t)/C_0 \text{ x } 100 \quad (2)$$

where C_0 is the initial concentration of the analyte, proportional to the absorbance measured with UV-HPLC, and C_t is the concentration measured at time t, after leaving the solution in contact with the hydrogel under irradiation (30 min-4 h).

2.5 | Recyclability Tests

Absorption and photodegradation experiments were performed, at the end of which the remaining solution was removed and substituted with Milli Q water for the overnight desorption. The obtained clean hydrogel was used for new adsorption and photodegradation tests, as described above. From the second to the sixth cycle, the experiments were performed consecutively in the same way.

2.6 | Analysis of Degradation Products

The solution obtained at the end of a photodegradation test was subjected to ^{1}H NMR and mass spectroscopy, in order to identify the chemical nature of the contained chemical species.

^{1}H NMR experiments were performed on a Bruker Ascend spectrometer (frequency: 400.13 MHz for 1H) (Billerica, MA).

For data processing, TopSpin 4.3.0 was used. NMR samples were prepared in a 5 mm NMR tube with a final concentration of 10^{-3} (or 10^{-5}) M and a volume of 500 µL, using a 90/10 original sample: D_2O mixture. The water 1H signal was suppressed by using an excitation sculpting with perfect echo (Bruker library: zgesgppe) pulse sequence, with standard parameters.

Mass spectra were recorded by direct infusion on a Thermo Fisher Scientific (Waltham, MA) LCQ Fleet ion trap spectrometer and processed with Qual Browser Thermo Xcalibur 4.0.27.13. The instrument was set both in negative and positive ionization modes to acquire different spectra, with a sheath gas flow rate = 8, auxiliary gas flow rate = 0, sweep gas flow rate = 0, 4.5 kV spray voltage, 250°C capillary temperature, and a flow rate of 5 µL/min. The samples were diluted 1:10 in MeOH before the infusion to a final concentration of 100 nM.

3 | Results and Discussion

The outline of the experimental preparation of chitosan and composite chitosan/TiO_2 hydrogels and the assessment of their performance in adsorption, recovery, and sunlight-driven photodegradation of SMX in mineral water is shown in Figure 1a.

3.1 | Characterization of the Chitosan-Based Hydrogels

By exploiting the pH-dependent solubility of chitosan, chitosan was first dissolved in aqueous acetic acid solutions, while hydrogel formation was induced by subsequent crosslinking in the presence of NaOH, leading to the formation of physical hydrogels. For the preparation of CH/TiO_2 hydrogels, a TiO_2 suspension in acetic acid was initially prepared, followed by the addition of chitosan to ensure homogeneous incorporation of the photocatalyst within the polymeric network. Figure 1b,c shows SEM images of the TiO_2 nanoparticles dispersed within the gel matrix. The identification of the TiO2 particles was confirmed by EDX analysis (see the inset of Figure 1c). The incorporation of TiO_2 nanoparticles into the acidic chitosan solution significantly increased the viscosity of the precursor and influenced the final morphology of the resulting hydrogels. In particular, the presence of TiO_2 led to thicker structures and induced a distinct color change, as the hydrogels turned white.

To gain insights into the chemical composition of the obtained hydrogels and verify the effective embedding of TiO_2 nanoparticles, both Fourier transform infrared (FTIR) and Raman analyses were performed. The effective incorporation of TiO_2 within the chitosan matrix was confirmed by Raman spectroscopy (Figure 2a). The spectrum of the CH/TiO_2 hydrogel exhibits the characteristic features of anatase (A), with peaks centered at 398 cm^{-1} (E_g), 517 cm^{-1} (A_{1g},+B_{1g}), and 639 cm^{-1} (E_g), together with a peak at 447 cm^{-1} characteristic of the rutile phase (R). This is consistent with the fact that Degussa P25 TiO_2 is a mixture of anatase and rutile phases and confirms that the nanoparticles were effectively incorporated within the gel matrix [23]. Furthermore, the vibrational modes of chitosan (CH) at 1100 cm^{-1} (representative of the glucosidic backbone, C—O—C/C—O/C—OH stretching), 1644 cm^{-1} (amide I, C═O), 2889 cm^{-1} (C—H stretching) and a broad band between 3000 and 3600 cm^{-1} (O—H and N-H stretching) are not significantly affected by the presence of TiO_2, as demonstrated by the similarity with the spectral features of the CH hydrogel. These data are further confirmed by the ATR-IR investigation. Figure 2b displays the characteristic absorption bands of chitosan functional groups: —N—H and —OH stretching at 3413, 3281,3166 cm^{-1}, —C═O stretching at 1642 cm^{-1} (amide I), N-H bending and C-N stretching at 1551 cm^{-1} (amide II), C—N stretching and N-H bending at 1334 cm^{-1} (amide III), —CH_2 bending at 1377 cm^{-1}, and —C—O—C stretching, C—O stretching at 1112, 1075 and 1022 cm^{-1} (characteristic of polysaccharides). As for Raman analyses, no significant shifts or intensity changes were observed between CH and CH/TiO_2 hydrogels, indicating that the incorporation of TiO_2 NPs does not alter the chemical structure of the chitosan backbone, confirming that the nanoparticles are physically embedded within the hydrogel matrix.

3.2 | Adsorption and Photodegradation Tests

In order to quantify the adsorption capability of the composite hydrogels, a disk of 1.1 g was immersed in 5 mL of a 10^{-5} M SMX solution overnight, and the variation in pollutant concentration before and after passive adsorption was evaluated using UV-HPLC. The adsorption performance was calculated using Equation (1). It is important to underline that the SMX solution was made using mineral water to increase the complexity of the system, making it closer to reality, and verify if the presence of ions could interfere with hydrogel adsorption. The adsorption efficiency of hydrogels functionalized with TiO_2 (CH/TiO_2) was compared with that of pure chitosan hydrogel (CH), as shown in Figure 3a. The overnight adsorption for CH was 17.28 ± 1.92% and 17.64 ± 4.90% for CH/TiO_2. These results demonstrate that the chitosan hydrogel matrix is mainly responsible for the adsorption processes, but the incorporation of TiO_2 does not significantly reduce it. Similar adsorption capability is maintained when the concentration of SMX solution is increased to 10^{-3} M. This observation suggests that the key factor that rules the maximum adsorption capability of the hydrogels is the partition equilibrium between the hydrogel (entrapped water) and solution (free water), and there are no significant specific interactions between the chitosan network and SMX molecules. Two major points should be highlighted in this regard. First, the adsorption tests were carried out at near-neutral conditions. Literature reports that pH influences the adsorption efficiency, as well as the type of transformation products achieved upon radical-assisted degradation of SMX [25–27]. However, the aim of the present study is to assess the performances of the composite gels in real working conditions, avoiding any pre-treatment of water. As will be discussed later, these materials are intended to be applied for outdoor, point-of-use remediation, where the pH is that of mineral water (lakes, rivers, in general any freshwater streams). For the same reason, all the experiments were carried out in the presence of cationic and anionic species that are commonly found in mineral water, to assess any possible interferences. These results demonstrated that these gels are not negatively affected by the presence of these species.

Upon 4 h of solar light irradiation, the concentration of SMX in solution in presence of CH/TiO_2 hydrogel is significantly reduced, and the removal efficiency of CH/TiO_2 hydrogel reaches a value

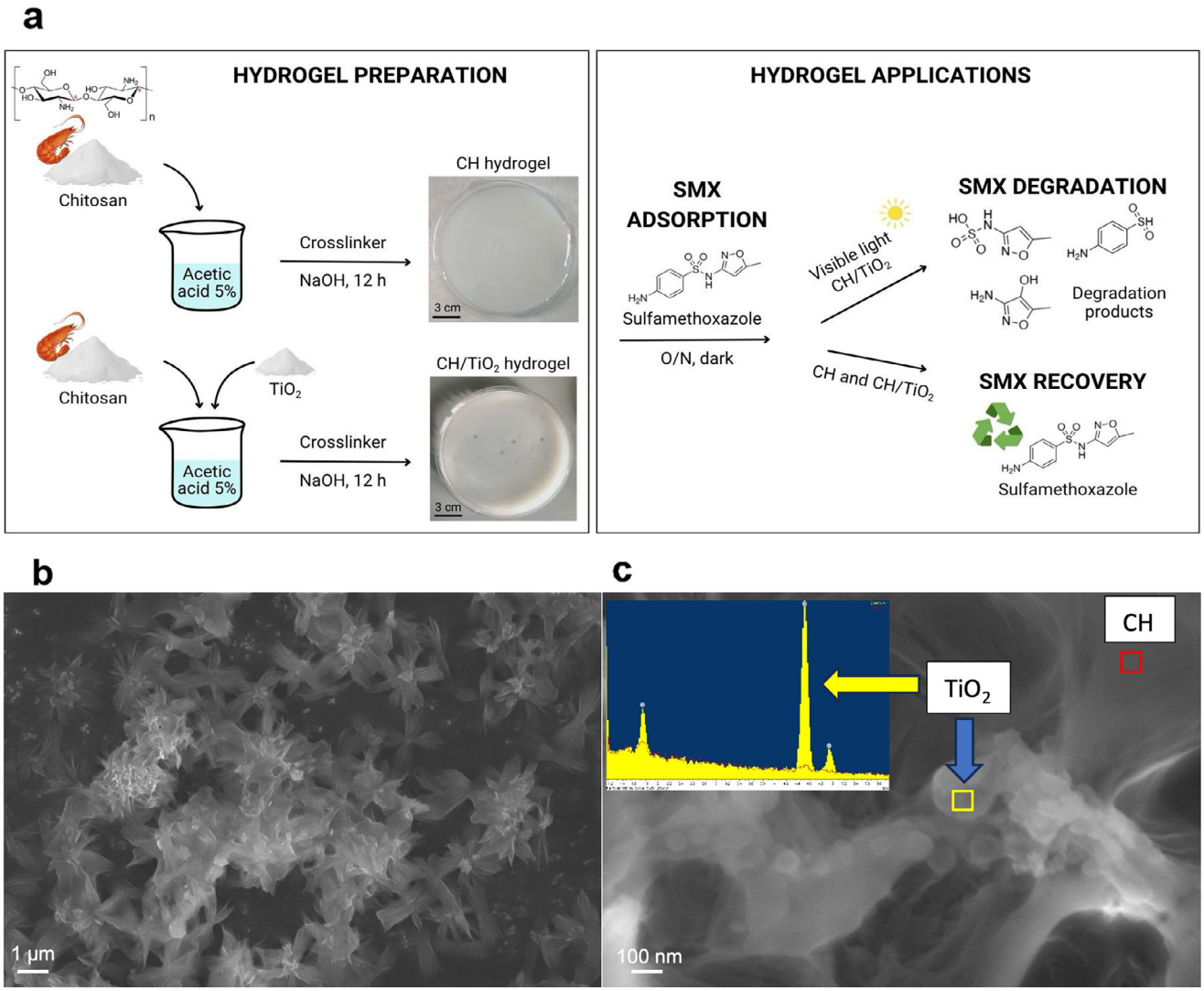

FIGURE 1 | Experimental scheme illustrating the preparation of chitosan (CH) and chitosan/TiO_2 (CH/TiO_2) hydrogels and their application in SMX adsorption, recovery, and/or sunlight-driven photodegradation. SEM images at low (b) and high (c) magnification of the interior of a dried CH/TiO_2 hydrogel, with EDX analysis in the inset, comparing two selected regions: one containing (yellow) and one without TiO_2 nanoparticles.

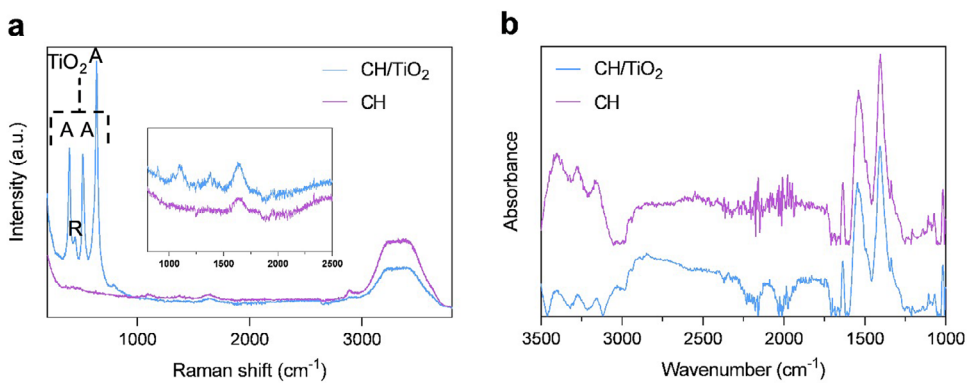

FIGURE 2 | Characterization of the CH and CH/TiO_2 hydrogels: (a) Raman spectra of wet chitosan hydrogels with (blue) or without (violet) TiO_2 nanoparticles; (b) FTIR-ATR spectra of dry chitosan hydrogels with (blue) or without (violet) TiO_2 nanoparticles.

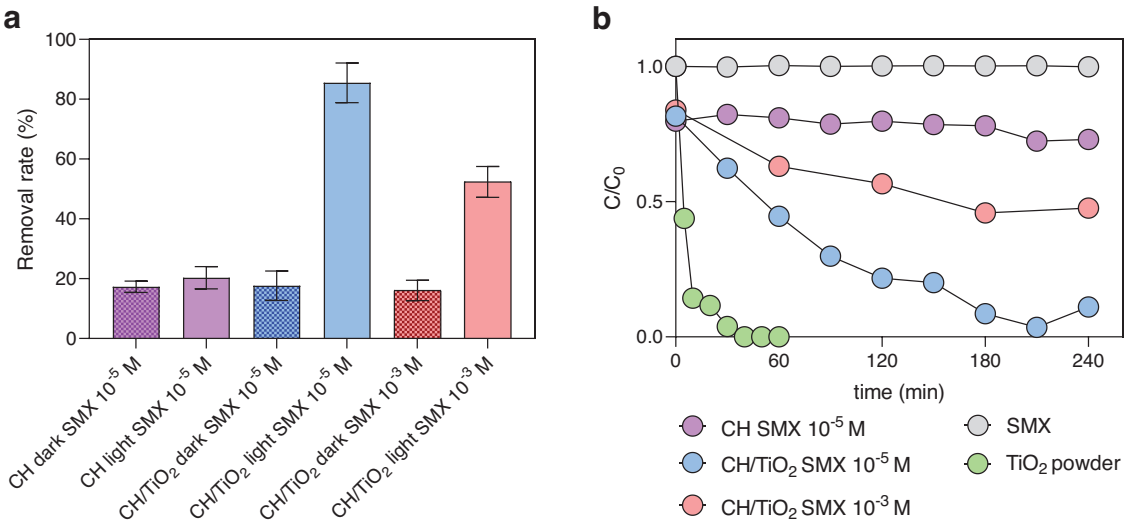

FIGURE 3 | (a) Comparison between adsorption capability and photocatalytic capability, after 4 h of irradiation under solar simulator, toward SMX 10^{-5} and 10^{-3} M of CH and CH/TiO_2 hydrogels; (b) Comparison of the photodegradation activity under solar simulator of CH (pink) and CH/TiO_2 (blue) toward SMX 10^{-3} M and CH/TiO_2 (red) toward SMX 10^{-3} M. SMX self-degradation (grey) under solar light and the photodegradation activity of TiO_2 powder toward SMX 10^{-5} M (green) are included as reference. Error bars are within the experimental point size.

of 85.48 ± 6.61% for the 10^{-5} M SMX solution and a value of 52.3618 ± 5.16% for the 10^{-3} M SMX solution, suggesting that CH/TiO_2 hydrogels are characterized by a significant photocatalytic activity. Systematic photocatalytic tests allowed this effect to be investigated in more detail.

The variation of the concentration of SMX upon irradiation by a solar simulator at an irradiance of 1 sun for 4 h in the presence of different types of hydrogels is shown in Figure 3b. First of all, it is visible that both the self-degradation of SMX and the degradation of SMX by CH hydrogels are negligible since the removal of SMX from water for CH hydrogels is only caused by adsorption. During the photoirradiation, the hydrogels remained stable, and the removal of SMX from water for the CH hydrogel is only caused by adsorption.

On the other hand, the presence of TiO_2 confers to the hydrogel system a photodegradation activity. The photocatalytic activity of TiO_2 relies on the production of e^-/h^+ pairs upon absorption of light with energy commensurate with the optical bandgap, which is around 3 eV. According to previous studies on analogous systems, the photogenerated holes (h^+) are able to promote the oxidation of the pollutant through the generation of $^{\bullet}OH$ species, whereas the photogenerated electrons (e^-) can reduce atmospheric O_2 to produce $^{\bullet}O_2^-$ species [16, 24–36]. The employed TiO_2 is undoped, thus the photoactivity is supposed to be mainly promoted by the UV, which is only a small portion (4%–5%) of solar irradiation. The efficiency of photodegradation depends on the concentration of the initial solution: SMX removal is less efficient at higher concentration (10^{-3} M) and more efficient at lower concentration (10^{-5} M). These results mirror the overall process of SMX abatement. In the dark, part of SMX has been distributed within the gel network, as shown by adsorption data. Upon irradiation, the SMX molecules within the gel are progressively degraded by radical species produced by TiO_2, and new SMX molecules can be uptaken from solution to continue the process [24]. The small oscillations of SMX concentration observed during irradiation (for example, concentration data acquired after 240 min.) are probably due to the release of unreacted SMX from the gel. This dynamic diffusion-uptake-reaction-back diffusion process rules the efficiency of the pollutant removal, and the diffusion of SMX molecules from the solution toward the gel and the availability of TiO_2 active sites are the main limiting factors for the reaction rate. At the outset of the irradiation, the diffusion rate from the solution to the gel is high, driven by the concentration gradient generated by the consumption of SMX molecules within the gel. However, as the reaction proceeds, the kinetics progressively slow down, and the concentration of SMX inside the gel can become higher than that in solution. At this stage, part of the unreacted SMX molecules is released back to the solution to restore the equilibrium.

For a comparison, the same amount of TiO_2 contained in the composite hydrogel, but in the form of free powder were put in direct contact with the same volume of SMX solution (10^{-5} M). Figure 3b shows that the SMX removal process is accomplished within 30 min, which means that in the absence of gel matrix, the reaction could proceed about seven times faster. However, as we will deeply discuss later, in view of practical application, the lower efficiency of hydrogel systems is not a major limitation and is counterbalanced by other advantages in terms of safety (the TiO_2 catalyst is not released in water) and recyclability.

Finally, an experiment to compare the degradation under simulated solar light and real solar light irradiation was performed. A solution of SMX 10^{-5} M was put in contact with a hydrogel of CH/TiO_2 and exposed to the sunlight. After 4 h, the rate of degradation was 81.60 ± 0.86%, which is close to the degradation data obtained with the solar simulator (85.48 ± 6.61%). Thus, direct solar irradiation can effectively activate the system and promote the degradation of the SMX molecules.

Both under solar simulator and real sun, SMX photodegradation follows a first-order kinetics, characterized by rate constants

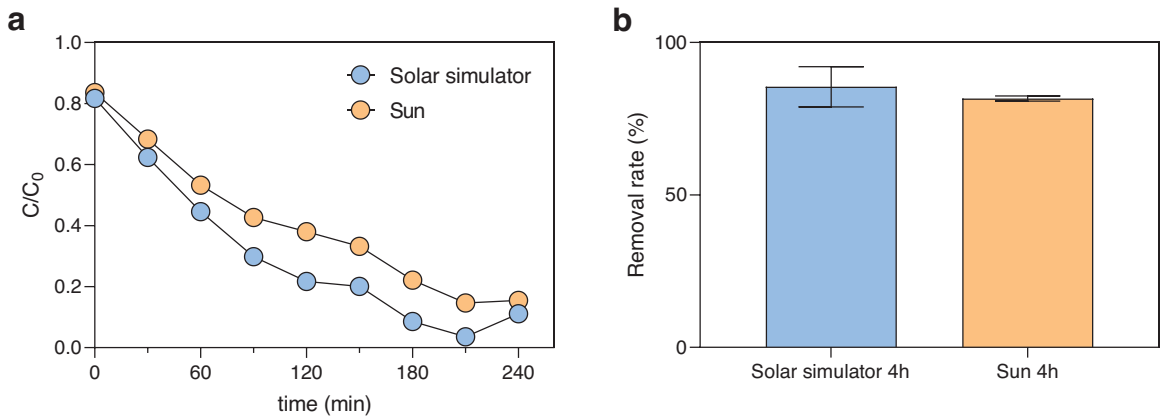

FIGURE 4 | (a) Comparison of the photodegradation activity under solar simulator (blue) and sunlight (orange) of CH/TiO_2. Error bars are within the experimental point size; (b) Comparison between the SMX 10^{-5} M removal efficiency after 4 h of irradiation under solar simulator (blue) and solar light (orange).

equal to 0.0112 min^{-1} (simulator) and 0.0074 min^{-1} (real sun) (Figure 4).

The photodegradation activity under direct solar light opens important perspectives in view of outdoor applications. In this regard, the most noteworthy aspect is related to the reduction of energy impact. Sunlight avoids the use of other light sources, which represents a constant drawback in terms of energy consumption. Although the reaction kinetics is far from that achievable using advanced oxidation processes integrated in water-treatment plant, like those involving plasma generated by dielectric breakdown discharge (DBD) [26, 27], which are very competitive in terms of energy efficiency, in the present case this does not represent a major issue, since the composite gels can be utilized outdoor as point-of-use tandem adsorbents/photocatalysts, without any particular time and processing constraints. Their stability and safety (*see* the next paragraph) would allow them to be placed in the location where they need to be utilized for an extended period of time, contributing to mitigating the concentration of antibiotics and, in general, emerging pollutants that will be conveyed into a treatment plant or, in the worst case, released in the environment.

3.3 | Recycling/Reuse and Safety Issues

The reusability of CH and CH/TiO_2 hydrogels, both for adsorption and photocatalysis, is a key factor in evaluating their cost-effectiveness and practical applicability in water treatment. After pollutant adsorption, the hydrogel can be removed from the solution using tweezers and subsequently resuspended in water. We tested the release of the adsorbed SMX in a volume of 5 mL Milli-Q water by measuring the concentration of SMX during an overnight incubation after the addition of a contaminated CH hydrogel disk. As shown in Figure 5a, SMX desorption is successfully and quantitatively achieved simply by soaking the contaminated CH hydrogel in Milli Q water, demonstrating that almost all the adsorbed pollutant is released overnight and can be recovered. Figure 5b presents the results of six consecutive reuse cycles, and the data indicate that only a slight decrease in adsorption efficiency for the CH hydrogel can be observed. In parallel, the recyclability of CH/TiO_2 hydrogels as an efficient photocatalyst was also studied, and the results are summarized in Figure 5c. Again, six consecutive cycles were performed, showing only a minor reduction in photocatalytic activity for the CH/TiO_2 hydrogel, suggesting only minimal deactivation. These results confirm the structural stability and functional reusability of both hydrogels as adsorbent and photocatalytic materials, respectively. To assess the suitability of these hydrogels for real application, we performed stability tests aimed at evaluating their resistance to illumination and microbial growth during prolonged storage under ambient conditions. During photoirradiation, all the tested hydrogels remained stable, preserving their shape and size even after six cycles of utilization. Figure S1 illustrates the evolution of chitosan hydrogels after 7 and 14 days of exposure to air, and compares their behavior with that of similar hydrogels based on another common biopolymer, alginate. While the alginate samples show evident microbial colonization, with progressive mold growth over time, the chitosan hydrogels remain intact and free of visible contamination. This remarkable difference highlights the intrinsic antimicrobial properties of chitosan, which effectively inhibit microbial proliferation, thereby enhancing the stability and durability of the material compared to alginate. TXRF analysis (Figure S2) was employed to directly assess the potential release of TiO_2 nanoparticles from the gel into the aqueous medium. The results showed no detectable titanium signals in the analyzed solutions, indicating that, within the detection limits of the technique, no TiO_2 release occurred. This result supports the effective immobilization of the nanoparticles within the gel matrix and confirms the material's stability upon contact with water. Importantly, preventing TiO_2 release is crucial for the applications of this kind of system, since uncontrolled dispersion of nanoparticles into water would not only compromise the catalytic performance of the system, but also contribute to secondary environmental contamination.

3.4 | Degradation Products Analysis

To elucidate the degradation mechanism and catalytic fragmentation pathway of SMX, NMR and ESI-MS analysis were performed. NMR analysis (Figure 6) showed that the photodegradation by

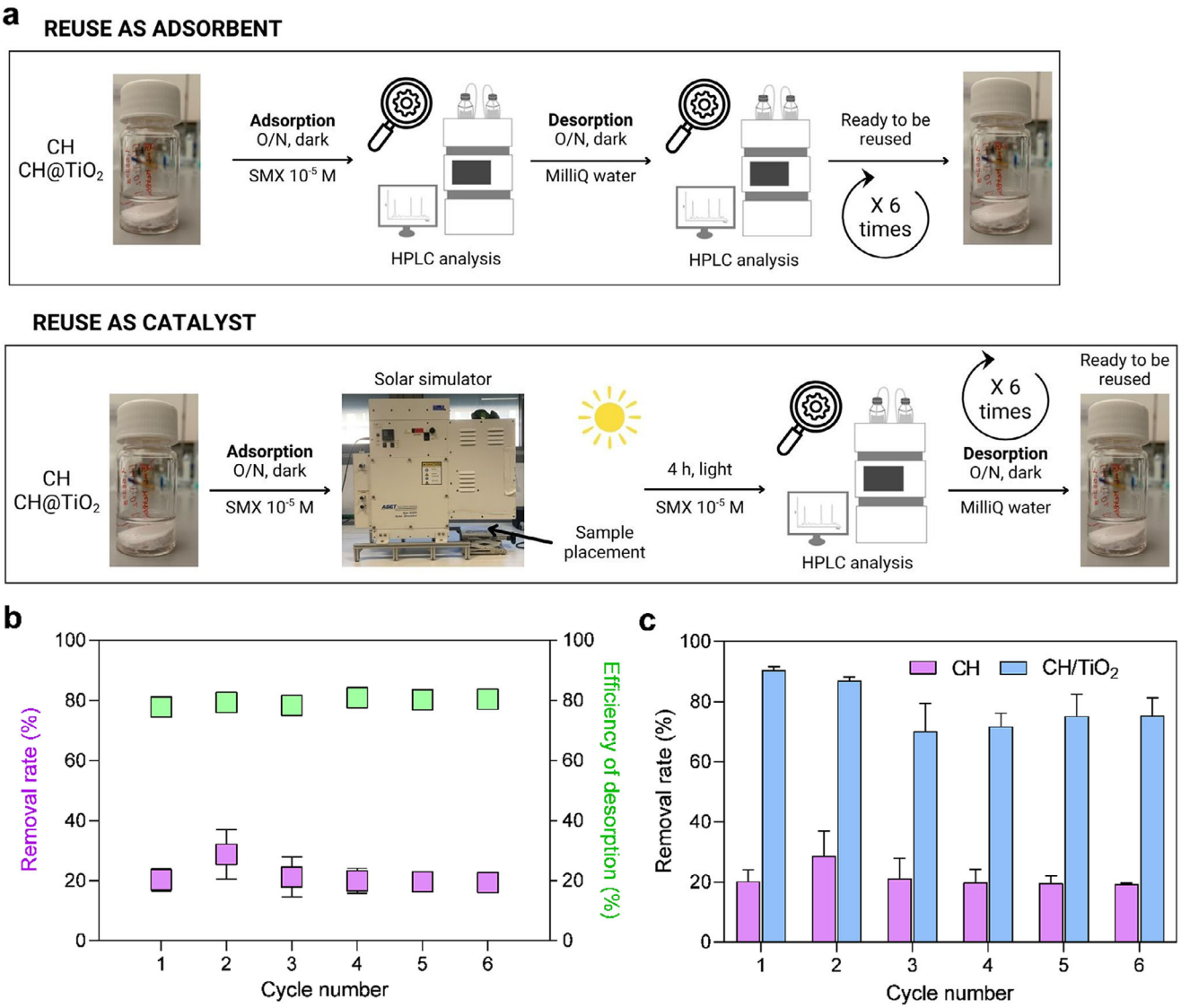

FIGURE 5 | SMX release and reusability of the hydrogels. (a) Schematic representation of the experimental procedure for hydrogel reuse as an adsorbent (top) and catalyst (bottom); (b) Comparison between SMX adsorption (pink) onto the CH hydrogel and its desorption in Milli-Q water (green). Error bars are within the experimental point size; (c) Adsorption and photocatalytic performances of CH (pink) and CH/TiO_2 (blue) hydrogels during SMX removal over six consecutive reuse cycles.

CH/TiO_2 hydrogels promotes the conversion of the molecule into other compounds, in particular, as can be observed in the reported spectra, while signals of sulfamethoxazole are still present, some new peaks appear, suggesting the formation of a new aromatic system and another methoxazole ring. This observation is in line with previous studies investigating degradation pathways of this compound [28, 29].

The ESI-MS analysis (Figure 7) further confirmed these results: the spectra acquired in positive and negative ionization mode showed the presence of several methoxazole-based degradation products and of a benzene sulfonamide, respectively. Again, these results are in agreement with literature data [25, 29–31].

The photo-induced generation of byproducts is a critical issue for all the remediation processes associated with the removal of emerging pollutants and deserves special attention. On one hand, further efforts should be addressed to the design and synthesis of specific (photo)catalysts that are able to completely mineralize the organic pollutants without damaging the hydrogel network. On the other hand, the possibility to generate and recover new small molecules originated from pollutants can open interesting perspectives for green chemistry and waste-to-treasure repurposing strategies [37].

4 | Conclusions

In this work, we assessed an integrated water remediation system that combines the photocatalytic activity of TiO_2 with the adsorption capability of a chitosan-based hydrogel in true-to-life conditions. We demonstrated that TiO_2 is effectively embedded inside the hydrogel matrix, limiting the risk of uncontrolled release of potentially harmful nanoparticles, and remains photoactive under both simulated and real solar light irradiation. SMX was chosen as an example of a pharmaceutical

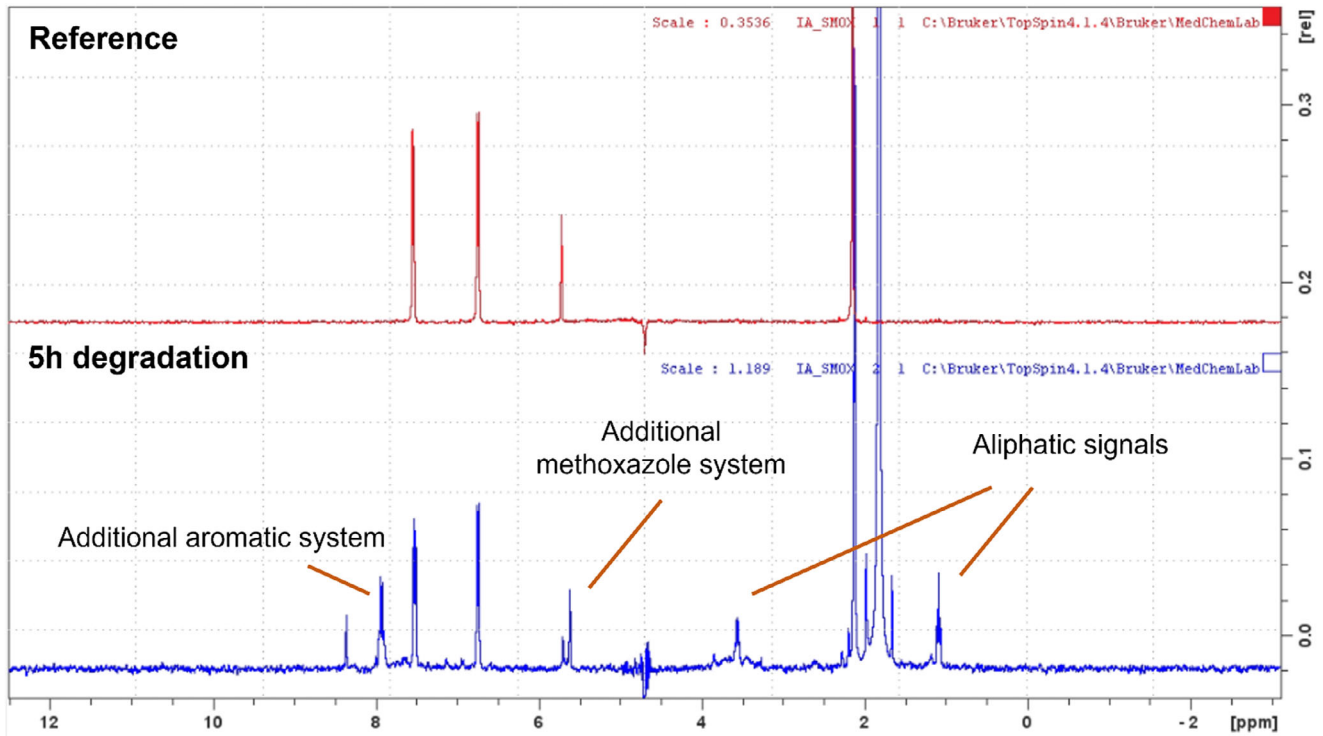

FIGURE 6 | NMR analysis showing the ^{1}H spectrum of sulfamethoxazole reference (red) in comparison with the sample after 5 h of photodegradation (blue).

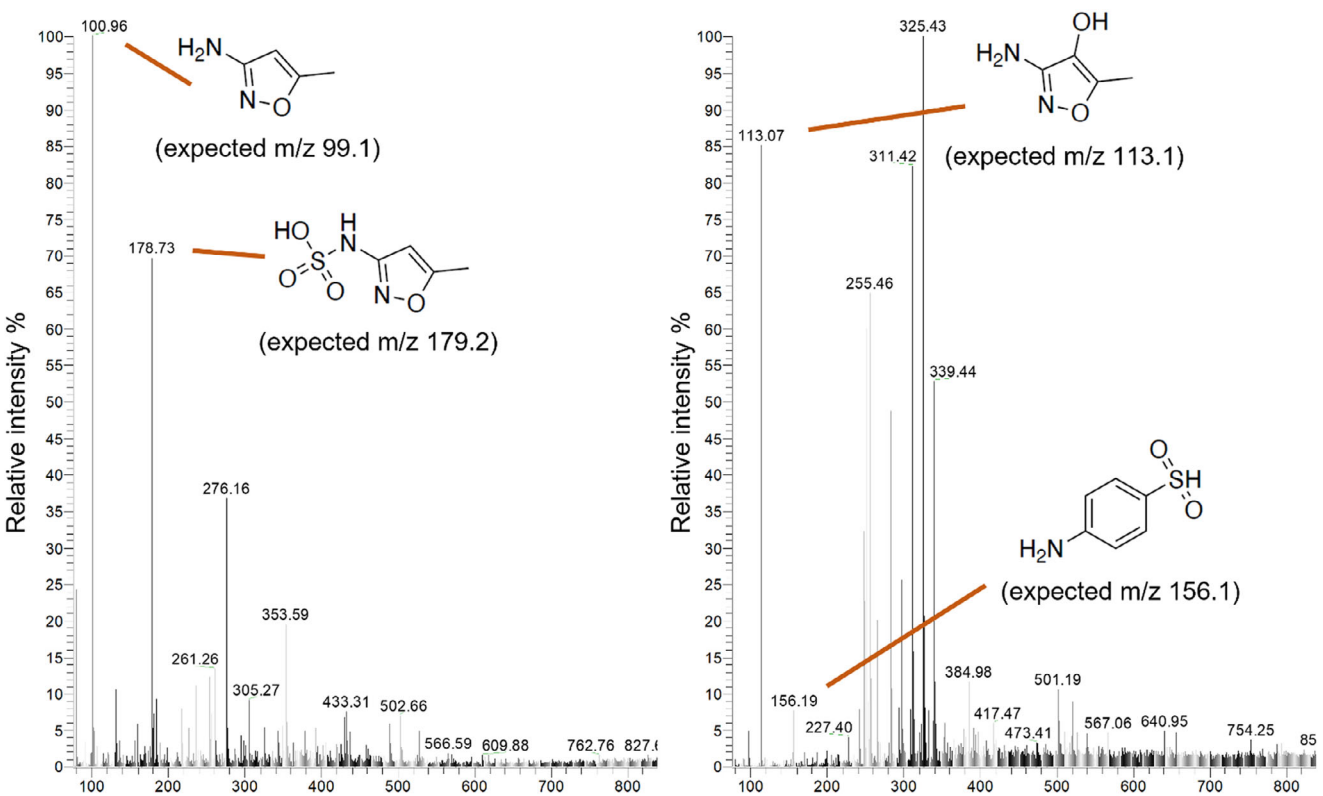

FIGURE 7 | ESI-MS analysis of the SMX solution after 5 h of photodegradation. In the left panel, the spectrum obtained through positive ionization is reported, while the right panel depicts the negative ionization spectrum. *Note:* chemical structures of neutral species have been reported.

contaminant, and its photodegradation proceeds under solar light while occurring simultaneously with adsorption. This results in a high overall removal efficiency (~85%). Furthermore, the system exhibits notable structural stability and reusability; it can be employed repeatedly (at least, 6 consecutive cycles) for both adsorption and photocatalysis without significant loss of performance. In particular, the composite hydrogels are not affected by microbial colonization and biofouling formation, and their adsorption/removal capability is maintained in mineral water, i.e., in ionic strength conditions that are commonly found in water courses.

Overall, the combination of recyclability, robustness, and efficient operation under real sunlight highlights the potential of this hybrid chitosan hydrogel-TiO_2 system for practical water treatment applications [38]. This system can set the basis for further development of more selective and efficient catalysts that will be able to achieve the complete mineralization of the emerging pollutants or their transformation into valuable products.

Author Contributions

B.C. performed formal analysis, investigation, methodology, validation, visualization, and writing of the original draft, as well as review and editing of the manuscript. G.R. contributed to methodology, validation, and writing – review and editing. A.G. was responsible for funding acquisition, methodology, validation, and writing – review and editing. M.F. carried out formal analysis of the SEM/EDX data. I.V. contributed through supervision and writing – review and editing. I.A. was involved in conceptualization, supervision, writing – review and editing, and funding acquisition.

Acknowledgements

The Authors acknowledge the use of instruments from the Proteomic Platform (Department of Molecular and Translational Medicine, Università di Brescia). The authors also acknowledge support from Regione Lombardia. This work has been accomplished within the framework of the project: "Rifiuti agroalimentari per la protezione delle piante (RiAPro)," funded by the Italian Ministry of Environment and Energy Security (MITE)/CUP: D83C23001580001.

Open access publishing facilitated by Universita degli Studi di Brescia, as part of the Wiley - CRUI-CARE agreement.

Conflicts of Interest

The authors declare no conflicts of interest.

Data Availability Statement

The data that support the findings of this study are available on request from the corresponding author. The data are not publicly available due to privacy or ethical restrictions.

References

1. WWAP (UNESCO World Water Assessment Programme), *The United Nations World Water Development Report 2019: Leaving No One Behind*, (WWAP UNESCO World Water Assessment Programme, 2019), 1–186.

2. Singh, K. K. Sodhi, N. V, et al., "Managing the Complexity of Emerging Contaminants in Aquatic Environments: Exploring Their Ecotoxicological Impacts, Detection Techniques, and the Use of Innovative Technologies for Their Remediation," *Discover Catalysis* 2, no. 1 (2025), https://doi.org/10.1007/s44344-025-00013-8.

3. K. Całus-Makowska, Ł. J. Binkowski, and A. Grobelak, "Pharmaceutical Residues in Wastewater Treatment Plants in Poland: Removal Efficiency and Risk Assessment," *Journal of Environmental Management* 394 (2025): 127480, https://doi.org/10.1016/j.jenvman.2025.127480.

4. M. Ahtasham Iqbal, S. Akram, S. Khalid, et al., "Advanced Photocatalysis as a Viable and Sustainable Wastewater Treatment Process: A Comprehensive Review," *Environmental Research* 253 (2024): 118947, https://doi.org/10.1016/j.envres.2024.118947.

5. J. B. Adeoye, Y. H. Tan, S. Y. Lau, et al., "Advanced Oxidation and Biological Integrated Processes for Pharmaceutical Wastewater Treatment: A Review," *Journal of Environmental Management* 353 (2024): 120170, https://doi.org/10.1016/j.jenvman.2024.120170.

6. F. C. Moreira, R. A. R. Boaventura, E. Brillas, and V. J. P. Vilar, "Electrochemical Advanced Oxidation Processes: A Review on Their Application to Synthetic and Real Wastewaters," *Applied Catalysis B: Environmental* 202 (2017): 217–261, https://doi.org/10.1016/j.apcatb.2016.08.037.

7. S. Foorginezhad, M. M. Zerafat, A. F. Ismail, and P. S. Goh, "Emerging Membrane Technologies for Sustainable Water Treatment: A Review on Recent Advances," *Royal Society of Chemistry* 4 (2025): 530–570, https://doi.org/10.1039/d4va00378k.

8. S. Javaid, A. Zanoletti, A. Serpe, E. Bontempi, I. Alessandri, and I. Vassalini, "Glassy Powder Derived from Waste Printed Circuit Boards for Methylene Blue Adsorption," *Molecules* 29, no. 2 (2024): 400, https://doi.org/10.3390/molecules29020400.

9. I. Vassalini, G. Ribaudo, A. Gianoncelli, M. F. Casula, and I. Alessandri, "Plasmonic Hydrogels for Capture, Detection and Removal of Organic Pollutants," *Environmental Science: Nano* 7, no. 12 (2020): 3888–3900, https://doi.org/10.1039/D0EN00990C.

10. I. Vassalini, N. Bontempi, S. Federici, M. Ferroni, A. Gianoncelli, and I. Alessandri, "Cyclodextrins Enable Indirect Ultrasensitive Raman Detection of Polychlorinated Biphenyls Captured by Plasmonic Bubbles," *Chemical Physics Letters* 775 (2021): 138674, https://doi.org/10.1016/j.cplett.2021.138674.

11. A. Boontanom, M. Maddaloni, P. Suwanpinij, I. Vassalini, and I. Alessandri, "Industrial Waste Against Pollution: Mill Scale-Based Magnetic Hydrogels for Rapid Abatement of Cr(VI)," *Environmental Science: Water Research & Technology* 10, no. 2 (2024): 551–564, https://doi.org/10.1039/d3ew00490b.

12. J. Gjpalaj and I. Alessandri, "Easy Recovery, Mechanical Stability, Enhanced Adsorption Capacity and Recyclability of Alginate-based TiO_2 Macrobead Photocatalysts for Water Treatment," *Journal of Environmental Chemical Engineering* 5, no. 2 (2017): 1763–1770, https://doi.org/10.1016/j.jece.2017.03.017.

13. I. Vassalini, J. Gjipalaj, S. Crespi, et al., "Alginate-Derived Active Blend Enhances Adsorption and Photocatalytic Removal of Organic Pollutants in Water," *Advanced Sustainable Systems* 4, no. 7 (2020): 201900112, https://doi.org/10.1002/adsu.201900112.

14. B. C. Nguyen, T. M. Truong, N. T. Nguyen, D. N. Dinh, D. Hollmann, and M. N. Nguyen, "Advanced Cellulose-Based Hydrogel TiO_2 Catalyst Composites for Efficient Photocatalytic Degradation of Organic Dye Methylene Blue," *Scientific Reports* 14, no. 1 (2024): 10935, https://doi.org/10.1038/s41598-024-61724-w.

15. B. Taghiloo, A. Shahnazi, and M. R. Nabid, "Construction of Nanocomposite Hydrogel by TiO_2-Carbon Quantum Dots Encapsulated in Alginate with a Highly Efficient Adsorption and Photodegradation of Dye Pollutants," *Journal of Alloys and Compounds* 1005 (2024): 175859, https://doi.org/10.1016/j.jallcom.2024.175859.

16. K. Shang, R. Morent, N. De Geyter, Y. Wang, and Z. Yang, "Plasma Catalytic Degradation of Sulfamethoxazole in Water with Fe/Mn-LDO Catalyst: Perfomance and Mechanism," *Separation and Purification Technology* 360 (2025): 131145, https://doi.org/10.1016/j.seppur.2024.131145.

17. N. Kumar, R. Gusain, S. Pandey, and S. S. Ray, "Hydrogel Nanocomposite Adsorbents and Photocatalysts for Sustainable Water Purification,"

Advanced Materials Interfaces 10 (2023), 202201375, https://doi.org/10.1002/admi.202201375.

18. A. Balakrishnan, S. Appunni, and K. Gopalram, "Immobilized TiO_2/Chitosan Beads for Photocatalytic Degradation of 2,4-dichlorophenoxyacetic Acid," *International Journal of Biological Macromolecules* 161 (2020): 282–291, https://doi.org/10.1016/j.ijbiomac.2020.05.204.

19. M. Maddaloni and I. Vassalini, "Green Routes for the Development of Chitin/Chitosan Sustainable Hydrogels," *Sustainable Chemistry* 1, no. 3 (2020): 325–344, https://doi.org/10.3390/suschem1030022.

20. I. Vassalini, M. Maddaloni, M. Depedro, A. De Villi, M. Ferroni, and I. Alessandri, "From Water for Water: PEDOT:PSS-Chitosan Beads for Sustainable Dyes Adsorption," *Gels* 10, no. 1 (2024): 10010037, https://doi.org/10.3390/gels10010037.

21. M. Rinaudo, "Chitin and Chitosan: Properties and Applications," *Progress in Polymer Science* 31 (2006): 603–632, https://doi.org/10.1016/j.progpolymsci.2006.06.001.

22. V. Rilstone, Y. Filion, and P. Champagne, "Study on the Persistence of Ciprofloxacin and Sulfamethoxazole in Simulated Drinking Water Systems," *Environmental Systems Research* 14, no. 1 (2025), https://doi.org/10.1186/s40068-025-00396-5.

23. N. Zhai, K. V. Thomas, J. Li, and J. W. O'Brien, "Environmental Antimicrobial Resistance: Current Status and Future Prospects," *Environmental Contamination: Causes and Solutions* 1, no. 1 (2025): 2510001699, https://doi.org/10.53941/eccs.2025.100006.

24. D. G. J. Larsson and C. F. Flach, "Antibiotic Resistance in the Environment," *Nature Reviews Microbiology* 20, no. 5 (2022): 257–269, https://doi.org/10.1038/s41579-021-00649-x.

25. E. Lien, R. S. Sahu, W. L. Chen, and Y.-H. Shih, "Effective Photocatalytic Degradation of Sulfamethoxazole Using Tunable $CaCu_3Ti_4O_7$ Perovskite," *Chemosphere* 294 (2022): 133744, https://doi.org/10.1016/j.chemosphere.2022.133744.

26. E. Borowska, E. Felis, and K. Miksch, "Degradation of Sulfamethoxazole Using UV and UV/H_2O_2 Processes," *Journal of Advanced Oxidation Technologies* 18 (2015): 69, https://doi.org/10.1515/jaots-2015-0109.

27. X. Liu, C. Akay, J. Köpke, S. Kümmel, H. H. Richnow, and G. Imfeld, "Direct Phototransformation of Sulfamethoxazole Characterized by Four-Dimensional Element Compound Specific Isotope Analysis," *Environmental Science & Technology* 58, no. 23 (2024): 10322–10333, https://doi.org/10.1021/acs.est.4c02666.

28. N. Bouanimba, N. Laid, R. Zouaghi, and T. Sehili, "A Comparative Study of the Activity of TiO_2 Degussa P25 and Millennium PCs in the Photocatalytic Degradation of Bromothymol Blue," *International Journal of Chemical Reactor Engineering* 16, no. 4 (2018), https://doi.org/10.1515/ijcre-2017-0014.

29. I. Alessandri and I. Vassalini, "Oxygen-Mediated Surface Photoreactions: Exploring New Pathways for Sustainable Chemistry," *ChemPhotoChem* 7 (2023): 202300069, https://doi.org/10.1002/cptc.202300069.

30. A. Kutuzova, T. Dontsova, and W. Kwapinski, "Application of TiO_2-Based Photocatalysts to Antibiotics Degradation: Cases of Sulfamethoxazole," *Trimethoprim and Ciprofloxacin Catalysts* 11, no. 6 (2021): 728, https://doi.org/10.3390/catal11060728.

31. Y. Li, X. Zhao, Y. Yan, et al., "Enhanced Sulfamethoxazole Degradation by Peroxymonosulfate Activation With Sulfide-Modified Microscale Zero-Valent Iron (S-mFe0): Performance, Mechanisms, and the Role of Sulfur Species," *Chemical Engineering Journal* 376 (2019): 376, https://doi.org/10.1016/j.cej.2019.03.178.

32. K. Shang, R. Morent, N. Wang, et al., "Degradation of Sulfamethoxazole (SMX) by Water Falling Film DBD Plasma/Persulfate: Reactive Species Identification and Their Role in SMX Degradation," *Chemical Engineering Journal* 431 (2022): 133916, https://doi.org/10.1016/j.cej.2021.133916.

33. S. Zhao, C. Hou, L. Shao, W. An, and W. Cui, "Adsorption and In-Situ Photocatalytic Synergy Degradation of 2,4-Dichlorophenol by Three-Dimensional Graphene Hydrogel Modified with Highly Dispersed TiO_2 Nanoparticles," *Applied Surface Science* 590 (2022): 153088, https://doi.org/10.1016/j.apsuc.2022.153088.

34. C. Chen, S. Wang, F. Han, X. Zhou, and B. Li, "Synergy of Rapid Adsorption and Photo-Fenton-Like Degradation in CoFe-MOF/TiO_2/PVDF Composite Membrane for Efficient Removal of Antibiotics from Water," *Separation and Purification Technology* 333 (2024): 125942, https://doi.org/10.1016/j.seppur.2023.125942.

35. S. Wang, C. Chen, F. Han, X. Zhou, and B. Li, "In-Situ Construction of Nitrogen-Doped Porous Carbon Nanosheets Supported Well-Dispersed Fe_3O_4 Nanoparticles for Efficient Purification of Antibiotic Wastewater Via Peroxydisulfate Activation," *Colloids and Surfaces A: Physicochemical and Engineering Aspects* 684 (2024): 133139, https://doi.org/10.1016/j.colsurfa.2023.133139.

36. M. Salmistraro, A. Schwartzberg, W. Bao, et al., "Triggering and Monitoring Plasmon-Enhanced Reactions by Optical Nanoantennas Coupled to Photocatalytic Beads," *Small* 9 (2013): 3301–3307, https://doi.org/10.1002/smll.201300211.

37. A. Wołos, D. Koszelewski, R. Roszak, et al., "Computer-Designed Repurposing of Chemical Wastes Into Drugs," *Nature* 604, no. 7907 (2022): 668–676, https://doi.org/10.1038/s41586-022-04503-9.

38. X. Xu, J. Qiu, Z. Li, et al., "A Bifunctional Polyacrylamide-Alginate-TiO_2 Hydrogel Solar Evaporator for Integrated High-Efficiency Desalination and Photocatalytic Degradation," *Desalination* 611 (2025): 118920, https://doi.org/10.1016/j.desal.2025.118920.

Supporting Information

Additional supporting information can be found online in the Supporting Information section.

Supporting File: admi70544-sup-0001-SuppMat.docx.